Accepted Manuscript

Slow cycling intestinal stem cell and Paneth cell responses to Trichinella spiralis infection

Tanvi Javkar, Kevin R. Hughes, Fred Sablitzky, Jerzy M. Behnke, Yashwant R. Mahida

PII: S1383-5769(18)30421-5
DOI: https://doi.org/10.1016/j.parint.2019.05.001
Reference: PARINT 1923

To appear in: *Parasitology International*

Received date: 19 October 2018
Revised date: 21 March 2019
Accepted date: 1 May 2019

Please cite this article as: T. Javkar, K.R. Hughes, F. Sablitzky, et al., Slow cycling intestinal stem cell and Paneth cell responses to Trichinella spiralis infection, Parasitology International, https://doi.org/10.1016/j.parint.2019.05.001

Slow cycling intestinal stem cell and Paneth cell responses to *Trichinella spiralis* infection

Tanvi Javkar[1]; Kevin R Hughes[1]; Fred Sablitzky[2]; Jerzy M Behnke[2], Yashwant R Mahida[1,*]
yash.mahida@nottingham.ac.uk

[1]Nottingham Digestive Diseases Centre, University of Nottingham, Queen's Medical Centre, Nottingham, NG7 2UH, UK
[2]School of Life Sciences, University of Nottingham, Nottingham, UK

[*]Corresponding author at: Nottingham Digestive Diseases Centre, Queen's Medical Centre, Nottingham, NG7 2UH, UK.

ABSTRACT

There is limited information regarding responses by slow cycling stem cells during *T. spiralis*-induced T-cell mediated intestinal inflammation and how such responses may relate to those of Paneth cells. Transgenic mice, in which doxycycline induces expression of histone 2B (H2B)-green fluorescent protein (GFP), were used. Following discontinuation of doxycycline ("chase" period), retention of H2B-GFP enabled the identification of slow cycling stem cells and long-lived Paneth cells. Inflammation in the small intestine (SI) was induced by oral administration of *T. spiralis* muscle larvae. Epithelial retention of H2B-GFP per crypt cell position (cp) was studied following immunohistochemistry and using the Score and Wincrypts program. Compared to non-infected controls, there was significant reduction in the number of H2B-GFP-retaining stem cells in *T. spiralis*-infected small intestines. H2B-GFP-retaining stem cells peaked at around cp 4 in control sections, but smaller peaks at higher cell positions (>10) were seen in sections of inflamed small intestines. In the latter, there was a significant increase in the total number of Paneth cells, with significant reduction in H2B-GFP-retaining Paneth cells, but a marked increase in unlabelled (H2B-GFP-negative) Paneth cells. In conclusion, following *T. spiralis*-infection, putative slow cycling stem cell numbers were reduced. A marked increase in newly generated Paneth cells at the crypt base led to higher cell positions of the remaining slow cycling stem cells.

Key words: stem cells; Paneth cells; *Trichinella spiralis*

INTRODUCTION

The intestinal crypt represents a unique collection of cells in which proliferation, differentiation and cell migration are organized in a linear fashion along the long axis of the crypt. The cellular organization and crypt cell constituents are regulated by a small number of stem cells of which two main populations have been identified in the murine small intestine(1-3). The frequently cycling crypt base columnar stem cells are intercalated between Paneth cells and have been characterized based on their expression of Lgr5. The second population is located above the Paneth cell zone, at around cell position (cp) 4 and these cells demonstrate heterogeneity in their characteristics. These cells have been characterized based on their expression of Bmi1 and mTert. They retain DNA label and a subpopulation are sensitive to low dose radiation, but the majority are slow cycling and resistant to low- and high-dose radiation-induced cell death (4-7). Studies suggest that the latter cells play a major role in epithelial regeneration following radiation-induced damage. Proliferating transit-amplifying cells are located above the cp4 stem cells and they differentiate into functionally distinct subpopulations of epithelial cells, such as absorptive enterocytes, Paneth cells, goblet cells and enteroendocrine cells. Whether the distinct functional characteristics of all the stem cells in specific locations in the crypt are inherently determined or the consequence of local environmental signals (from the niche) remains to be determined. Niche-derived components of the *Wnt*, *Bmp* and *Notch* signalling pathways regulate intestinal stem cell functions (1, 2) and their cellular sources include Paneth cells and myofibroblasts(3, 8-10).

Recent work has shown significant overlap in the expression of specific markers and plasticity in stem cell identity(2, 3). Currently, there is limited information regarding stem cell responses during distinct stages (initiation, progression, repair and resolution) of inflammatory responses. There is also significant interest in the role of Paneth cells in the pathogenesis of chronic inflammatory diseases such as Crohn's disease(11) and in chronic nematode infections such as those caused by human hookworms(12, 13).

Small intestinal inflammation induced by the nematode *T. spiralis* is characterized by Th2-type responses that occur around the time of significant worm burden, when there is also an increase in the numbers of Paneth and goblet cells, together with villus atrophy and crypt

hyperplasia(14-19). Following worm expulsion, the mucosal and epithelial morphology returns to normal (about 4 weeks after infection). Thus, this physiological model of parasite infection provides an opportunity to study stem cells during distinct and transient changes to the epithelium induced by T cell-mediated inflammatory responses. The aim of our studies was to investigate slow cycling intestinal stem cells and Paneth cells following infection with *T. spiralis*.

MATERIALS AND METHODS

Animals

Transgenic mice in which doxycycline induces expression of histone 2B (H2B)-green fluorescent protein (GFP) were used for these studies. TetOP-H2B-GFP mice were generated as previously described (kind gift from the Hock laboratory) (20, 21) using a transgene integration strategy developed previously in embryonic stem cells to mediate site-specific recombination and enabling predictable and temporal expression. Briefly, M2-rtTA (reverse tet-repressor) was placed under the control of the constitutive promoter, ROSA with histone 2B (H2B)-green fluorescent protein (GFP) expression being controlled from the Tet-operator. Presence of doxycycline in the drinking water allows binding of the M2-rtTA protein to the Tet-operator, driving expression of H2B-GFP such that doxycycline acts as a molecular switch to turn on/off the expression of H2B-GFP.

The mice were bred in-house (B6D2F1 background). Animals (both male and female) aged 7-10 weeks were administered 2 mg/ml of doxycycline (D9891, Sigma) along with 10 mg/ml of sucrose (S7903, Sigma) in sterile drinking water for 23 days to induce transgene expression. Doxycycline was replaced with normal drinking water on day 24 of the experiment. Following discontinuation of doxycycline ("chase" period), H2B-GFP is lost in cycling cells during multiple cell divisions, but the label is retained in cells that are cycling slowly (quiescent).

All mice were maintained and bred (B6D2F1 background) in the Bio-support unit at the University of Nottingham with 12 hour light cycle (lights on between 7.00 am and 7.00 pm); animals were fed standard chow and water, *ad libitum* and all appropriate measures were undertaken to minimise pain or discomfort. The experiments were carried out in accordance with the UK Regulation of Animals (Scientific Procedures) Act of 1986.

Parasitological technique and tissue collection

Naïve BALB/c host mice (Charles River Ltd. Margate, Kent, UK) were used to maintain and recover *T. spiralis* as previously described (22). TetOP-H2B-GFP mice were orally gavaged with 300 *T. spiralis* larvae (L1 stage) in 0.2% agar on day 2 of post-doxycycline chase period. Naïve mice (untreated) were used as controls. Experiments were designed such that mucosal samples were obtained on day 13 of infection, which coincided with day 14 chase period (Figure 1). An experiment in which mice were infected for 27 days (29 days post-doxycycline) was also undertaken. Worm counts were not routinely undertaken in these studies because this mouse model of infection has been extensively studied by our laboratory for a number of years (15-17, 19, 23) and we inferred from this experience and confirmation of the predicted mucosal morphological changes that worm expulsion was complete by day 27.

At the end of the experiment, intestinal samples were recovered and flushed with 10 ml of phosphate buffered saline (PBS) and fixed in 10% neutral buffered formalin saline at room temperature for 24 hours. Samples were subsequently dehydrated through an ethanol and xylene series and embedded in paraffin wax (24). Proximal small intestinal samples (defined as duodenum) were taken 2-3cm distal to the pyloric sphincter. Mid-point Small intestinal samples (defined as Jejunum) were taken from the mid-point of the small intestine as measured from pyloric sphincter to ileo-caecal junction. Distal small intestinal samples (defined as ileum) were taken 2-3cm proximal to the ileo-caecal junction.

Immunohistochemistry and Double Immunofluorescence

For immunohistochemical and immunofluorescence studies, 5 um thick bundled paraffin-embedded wax tissue block sections were used. After rehydrating the sections in xylene and alcohol, they were treated with an antigen unmasking solution (H-3300, Vector Laboratories) and microwaved. The endogenous peroxidase activity was quenched using 0.3% hydrogen peroxide (H/1750/17, Fisher Scientific) solution in methanol, and incubated for 30 minutes in a histology dish and washed in PBS. Sections were incubated with 1:500 anti-GFP antibody (600–401-215, Rockland) after blocking non-specific binding. 100 µl of Dako envision goat anti-rabbit secondary antibody (K4002, Dako) was used as secondary antibody before the sections were incubated in the peroxidase substrate (SK- 4100, Vector

Laboratories) to achieve desired level of colour reaction. Finally, the sections were stained with haematoxylin and eosin and mounted using DPX Mountant fluid (44581, Sigma).

Double immunofluorescence studies were performed using 1:50 goat anti-lysozyme (27958, Santa Cruz) and 1:500 anti-GFP as primary antibodies. FITC-conjugated anti-rabbit antibody (611-702-127, Rockland) and 1:1000 rhodamine-conjugated anti-goat antibody (605-700-125, Rockland) were used as secondary antibodies. VECTASHIELD® Mounting Medium with DAPI (H-1200, Vector Laboratories) was used before visualisation under fluorescence microscope.

Scoring, data presentation and statistical analysis

Following immunohistochemistry, H2B-GFP-retaining putative slow cycling stem cells, H2B-GFP-retaining Paneth and unlabelled Paneth cells (identified by the presence of granules in the cytoplasm) in sections of small intestine were assessed using the Score and Wincrypts program (25, 26). The specific cell types were identified and entered in a code form (keyboard character) in the Score program. Files created by the Score program were then entered into the WinCRYPTS© software for data analysis. Fifty half crypts per section were analysed up to crypt cell position 20. Crypts with a good base, visible Paneth cell granules, middle and top in the plane of the section, and a visible crypt lumen were selected. Cells were assigned a position along the crypt-villus axis, with cell number increasing sequentially up the crypt-villus axis and cell position 1 at the centre of the base of the crypt. The analyses were undertaken in a blinded fashion.

The mean number of labelled cells at a particular crypt cell position was expressed as the labelling index (LI). Whole crypt LI represents the mean number of labelled cells per 50 half crypts. All the data were plotted using the LI values generated by the WinCRYPTS program for each cell position in the crypt. Data for whole crypt labelling index and Paneth cells per 50 half crypts are presented as median (IQR) and Mann-Whitney U test was used to analyse differences between the two groups.

To identify significant differences in cell positions, between uninfected controls and *T. spiralis*-infected mice, extension of the median test (EMT, a function in WinCRYPTS© program) on successive groups was used, with $p<0.01$ at the relevant cell positions(27). These data are presented as labelling index values (mean cell number per crypt cell position).

For the main study (Figure 1), three independent experiments were undertaken in which the post-doxycycline chase period was 14 days and involved a total of 10-15 mice in the control group and 7-12 mice in the infected group (day 13 of *T. spiralis* infection). In one

experiment, only the duodenum of mice infected with *T. spiralis* for 27 days (n=5) was studied (on day 29 of the post-doxycycline chase period).

RESULTS

Slow cycling stem cells in the inflamed small intestine

As per our previous studies(17), small intestinal inflammation at day 13 post-infection with *T. spiralis* was associated with villus atrophy and crypt hyperplasia.

Immunohistochemical studies using sections from all three regions of the small intestine showed that, compared to non-infected controls, there was significant reduction in the number of H2B-GFP-retaining putative slow cycling stem cells at day 13 of infection with *T. spiralis* (when worm burden was high), which coincided with day 14 of post-doxycycline chase period [labelled cells per 50 half crypts: 0.90 (0.30-1.40)] vs [0.20 (0-0.70)], $p<0.0001$; Figure 2a]. Consistent with our previous studies(4), H2B-GFP-retaining putative stem cells peaked at around cp4 (couple of cell positions higher in the ileum) in non-infected controls. By contrast, smaller peaks at higher cell positions were seen for these cells in the *T. spiralis*-infected small intestine (Fig 2b-f).

Paneth cells in the inflamed small intestine

There was a significant increase in the total number of Paneth cells throughout the small intestine of mice infected with *T. spiralis* for 13 days [Paneth cells per 50 half crypts: 266.0 (243.0-300.0) vs 163.0 (140.0-191.0), $p<0.0001$; Figure 3a]. A subpopulation of Paneth cells retained H2B-GFP in control mice, but significantly lower numbers of such cells were seen in the parasite-infected small intestine [Paneth cells per 50 half crypts: 65.0 (46.0-74.0) vs 30.0 (12.0-48.0), $p<0.0001$; Figure 3b). By contrast, there was a marked increase in the number of unlabelled (H2B-GFP-negative) Paneth cells in infected mice [Paneth cells per 50 half crypts: 240.0 (208.0-272.0) vs 103.0 (77.0-131), $p<0.0001$; Figure 3c], reflecting newly generated Paneth cells during the chase period (when doxycycline was not available to induce expression of H2B-GFP).

Profiles of crypt cell positions showed that, in addition to their appearance at higher crypt positions, the increase in Paneth cell numbers (H2B-GFP-labelled or –unlabelled) occurred throughout the crypt (Figure 4a - c). The loss of H2B-GFP-retaining Paneth cells

(and their replacement by newly generated unlabelled Paneth cells) was most prominent at cp 1 - 3 (Figure 5a - c). It is of interest that in the duodenum, there was an increase in the number of H2B-GFP-retaining Paneth cells at cp 5 – 11 (Figure 5a), implying movement to higher cell positions of these long-lived cells. The increase in H2B-GFP-unlabelled Paneth cells (newly generated cells) occurred in all crypt cell positions (Figure 6a - c).

Slow cycling stem cells and Paneth cells following resolution of inflammation

By day 27 post-infection the worms had been expelled from the small intestine and the mucosal morphology had returned to normal. This was confirmed via assessment of villus height and crypt depth as described previously (17, 19). In studies using sections from the duodenum, H2B-GFP-retaining putative slow cycling stem cells were seen in a similar position to uninfected controls (at around cp 4) (Figure 7a). At this time point, total Paneth cell numbers in the infected duodenum had also decreased to values similar to those seen in uninfected control mice (Figure 7b) (16, 17).

DISCUSSION

Numerous studies have characterized two subpopulations of stem cells in the small intestine, the frequently cycling crypt base columnar stem cells and those located above the Paneth cell zone (at around cell position 4)(1-3). The Lgr5-expressing crypt base columnar stem cells are responsible for the turnover of the epithelium under steady state. Stem cells above the Paneth cell zone are slow cycling and may predominantly act as reserve stem cells that are activated following epithelial injury and post-irradiation loss (4, 28, 29). To our knowledge, investigation of these cells during inflammatory responses in the small intestine has not been reported previously.

In our studies, small intestinal inflammation was induced following infection with the parasite *T. spiralis*. In this model, which has been studied for many years, expulsion of *T. spiralis* is under the control of CD4+ T cells, via Th2 cytokines, especially IL-4 and IL-13(14). Previous studies have shown that there is an initial Th1-type response in mesenteric lymph node cells, followed by a Th2-type response around the time of worm expulsion(15, 23). Around the time of Th2 response, significant changes occur in the small intestinal mucosa and epithelial cells. These changes include villus atrophy, crypt hyperplasia and an

increase in Paneth and goblet cell numbers(15-17). Paneth cells granules, which contain antimicrobial peptides and proteins(30), are released into the small intestinal lumen around the time of worm expulsion(16). Goblet cells secrete mucin glycoproteins and other biologically active molecules such as trefoil factor 3 (also called intestinal trefoil factor) and resistin-like molecule (RELM) beta(14, 18, 19). Recent studies have reported an increase in tuft cells following worm infection and these cells have been shown to initiate type 2-cell mediated immunity (31, 32).

As expected from our previous studies(16, 17), there was a significant increase in the total number of Paneth cells, at day 13 after infection with *T. spiralis*. In contrast to other epithelial cell types, small intestinal Paneth cells normally have a longer life span, which (based on retention of H2B-GFP) may extend to 100 days or more(4). In the *T. spiralis*-infected small intestine, there was a decrease in the number of H2B-GFP-retaining Paneth cells but a marked increase in those cells that were unlabelled. This implies the loss of long-lived Paneth cells, together with a striking increase in the generation of new Paneth cells throughout the parasite-infected small intestine. The concurrent decrease in the number of H2B-GFP-retaining putative slow cycling stem cells (loss of labelled stem cells due to cell division) suggests their significant contribution to the generation of new Paneth cells. It is likely that the slow cycling stem cells also contribute to the increase in the number of goblet cells. Their contribution to the generation of other epithelial cells types (such as absorptive enterocytes) in the inflamed small intestine remains to be determined. Bmi-1 has been shown to mark the slow cycling stem cell population and that these cells are distinct from the mitotically active Lgr5 expressing population (33). Our previous attempts to reliably label Lgr5- and Bmi-1-expressing intestinal stem cells using immunohistochemical approaches and commercially available antibodies have been unsuccessful. However, our analysis using fluorescence activated cell sorting (FACS) has demonstrated that isolated H2B-GFP expressing stem cells co-express both markers at the transcriptional level (4). As such, we believe that identification using H2B-GFP provides a reliable marker for tracking the slow cycling stem cell population. We do however accept that since Lgr5-expressing crypt base columnar stem cells may also participate, future studies to determine the relative contributions of the two stem cell populations in the generation of new Paneth cells in the *T. spiralis*-infected small intestine will be of interest.

Compared to control mice, the remaining putative slow cycling stem cells were located in higher crypt cell positions in the inflamed small intestine. This is likely to be due to the increase in the number of Paneth cells at the crypt base. Consistent with this concept, we have previously shown that around a similar time of *T. spiralis* infection, proliferating transit-amplifying cells also move up the crypt-villus axis(17). Moreover, our previous studies have shown that at an early time point (day 2) after exposure to the infective stage of the parasite, there is a significant increase in proliferative cells in the crypts due to expansion of the late transit cell population. Around the time that the Paneth cell compartment has expanded (around day 12), there is a significant dampening in proliferation in the putative stem cells and early transient regions (cell positions 4 – 100) (17). Bacterial infection may also lead to changes in the small intestinal crypt with similarities to those seen following infection with *T. spiralis*. Thus, infection with *Salmonella enterica* serovar Typhimurium has been shown to be associated with an increase in the total number of Paneth cells and also proliferation in the transit amplifying region of the crypt (34).

In addition to differentiation along the secretory pathway, increased proliferation of stem cells and their transient daughter cells may represent an aspect of the host protective response against infection. In support of this contention, colonic infection by the parasite *Trichuris muris* has been shown to lead to increased epithelial cell proliferation and turnover (that is believed to enable removal of the worms from their epithelial environment) that was greater in resistant, compared to susceptible strains of mice (35).

Paneth cells have previously been shown to be an important source of niche signals for Lgr5-expressing crypt base columnar cells(8) but their role in regulating Bmi1-expressing slow cycling stem cells remains to be determined. It is possible that other neighbouring cells, such as a subpopulation of myofibroblasts, may contribute to the retention of the characteristics of the slow cycling stem cells. In this case, the position of the relevant subpopulation of myofibroblasts would also be expected to change in the inflamed mucosa. However, if the functional characteristics of the slow cycling stem cells are inherently determined, the change in their position may solely be due to an increase in the number of cells (Paneth cells) at the crypt base.

The appearance of H2B-GFP-labelled Paneth cells at cell positions 5 – 11 in the inflamed duodenum, but not other parts of the small intestine (Figure 5a) suggests region-

specific capacity for long-lived Paneth cells to change their location in the crypt. Following resolution of inflammation (27 days after *T. spiralis* infection), Paneth cell numbers decrease to levels similar to those in the control mice(16). It is of interest that the remaining H2B-GFP-labelled slow cycling stem cells returned to their original position at this time point.

Thus, at the time of significant worm burden, the transient increase in small intestinal Paneth cells in *T. spiralis*-infected mice is associated with a temporary change in position of H2B-GFP-retaining putative slow cycling stem cells and transit amplifying cells(17). This model of parasite infection therefore provides an opportunity to characterise cellular and molecular aspects of stem cells and their niche during T cell-mediated inflammatory changes in the small intestine.

ACKOWLEDGEMENTS

We wish to thank members of the Bio Support Unit for their help in undertaking these studies.

Funding

Tanvi Javkar was supported by the University of Nottingham, via International Research Excellence Scholarship.

Figure 1

Experimental plan of the study**.** Transgenic mice (represented by grey mouse) were given doxycycline (DOX) (represented by the bright green mouse) for 23 days, also known as "pulse" period. The black arrow represents day 0 of chase after discontinuation of DOX. The orange arrow represents the day of infection with *T. spiralis* larvae and the red arrow represents day of tissue collection, i.e. day 14 chase. The gradation in the mouse colour illustrates the loss of H2B-GFP label.

Figure 2

Fewer slow cycling stem cells and change in their position in *T. spiralis*-infected small intestine (SI). Mucosal samples were obtained from control (n=10-15) and *T. spiralis*-

infected (n=7-12); day 13) mice, on day 14 of post-doxycycline chase period. (a) H2B-GFP-retaining putative stem cell numbers (per 50 half crypts - whole crypt labelling index, median is shown by horizontal line) were reduced in the infected SI (***P*<0.01; ****P*<0.0001). (b) – (d) Labelling index analysis [mean cell number per crypt cell position (cp)] showed smaller peaks of H2B-GFP-retaining putative stem cells at higher cps in infected SI (horizontal line: *P*<0.01). (e) & (f) Representative anti-GFP immunohistochemical (e) and double immunofluorescent [(f); anti-GFP- green; anti-lysozyme – red] studies (arrow: H2B-GFP-retaining stem cell; arrowhead: H2B-GFP-retaining Paneth cell; *: unlabelled Paneth cell; #: goblet cell).

Figure 3

Increase in total Paneth cell population, but reduction in H2B-GFP-retaining Paneth cells in *T. spiralis*-infected small intestine (SI). Samples described in Figure 2 were used. (a) Throughout the infected SI, the total Paneth cell population was increased. (b) & (c) In infected SI, H2B-GFP-retaining Paneth cells were significantly reduced (b), but numbers of unlabelled (H2B-GFP-negative) Paneth cell were significantly increased (***P*<0.01; ****P*<0.001; *****P*<0.0001). The data are presented as median (IQR).

Figure 4

Labelling index profiles of all (both labelled and un-labelled) Paneth cells. The mean number of labelled cells at a particular crypt cell position was expressed as the labelling index. The frequency of both labelled (H2B-GFP-retaining) and unlabelled (non-H2B-GFP-retaining) Paneth cells at each cell position was determined using the Score and Wincrypts program. The labelling index indicates the frequency of a Paneth cell at each cell position normalised to the number of crypts scored in the duodenum (a), jejunum (b) and ileum (c). The labelling index profiles of uninfected controls (solid line) and mice infected with *T. spiralis* for 13 days (broken line) are shown. The horizontal line indicates where the labelling index was significantly (P<0.01) higher in infected mice.

Figure 5

Labelling index analysis of H2B-GFP-retaining Paneth cells in *T. spiralis*-infected small intestine (SI). The mean number of labelled cells at a particular crypt cell position was expressed as the labelling index There was a prominent loss of H2B-GFP-retaining Paneth

cells at cps 1-3 in all three regions of the infected SI (a – c), but significant increase in these cells at cps 5-11 in the infected duodenum (a). Horizontal line: $P<0.01$).

Figure 6

Labelling index profiles of unlabelled Paneth cells. The mean number of labelled cells at a particular crypt cell position was expressed as the labelling index The frequency of non-H2B-GFP-retaining Paneth cells at each cell position was determined using the Score and Wincrypts program. The labelling index indicates the frequency of non-H2B-GFP-retaining Paneth cell at each cell position normalised to the number of crypts scored in the duodenum (a), jejunum (b) and ileum (c). The labelling index profiles of uninfected controls (solid line) and mice infected with *T. spiralis* for 13 days (broken line) are shown. The horizontal line indicates where the labelling index was significantly ($P<0.01$) higher in infected mice.

Figure 7

Position of putative slow cycling stem cells following resolution of inflammation. Duodenal samples were obtained from control (n=5) and *T. spiralis*-infected (n=5; day 27) mice, on day 29 of post-doxycycline chase period. (a) Immunohistochemistry using anti-GFP antibody shows that the putative slow cycling (H2B-GFP-retaining) stem cells (arrowed) are at similar position (cell position 4) in both control and *T. spiralis*-infected sections of the duodenum. Unlabelled (asterix) and H2B-GFP-retaining (arrowhead) Paneth cells and goblet cells (#) are also present. (b) Labelling index profiles of total (both labelled and unlabelled) Paneth cells in sections of uninfected controls (solid line) and mice infected with *T. spiralis* for 27 days (dash line) shows similarity in numbers and positions of these cells in the crypt, in contrast to the changes seen on day 13 post-infection (Figure 4a).

REFERENCES

1. Potten CS, Gandara R, Mahida YR, Loeffler M, Wright NA. The stem cells of small intestinal crypts: where are they? Cell Prolif. 2009;42(6):731-50.
2. Gracz AD, Magness ST. Defining hierarchies of stemness in the intestine: evidence from biomarkers and regulatory pathways. Am J Physiol Gastrointest Liver Physiol. 2014;307(3):G260-73.
3. Barker N. Adult intestinal stem cells: critical drivers of epithelial homeostasis and regeneration. Nature reviews Molecular cell biology. 2014;15(1):19-33.
4. Hughes KR, Gandara RM, Javkar T, Sablitzky F, Hock H, Potten CS, et al. Heterogeneity in histone 2B-green fluorescent protein-retaining putative small intestinal stem cells at cell position 4 and their absence in the colon. Am J Physiol Gastrointest Liver Physiol. 2012;303(11):G1188-201.

5. von Furstenberg RJ, Buczacki SJ, Smith BJ, Seiler KM, Winton DJ, Henning SJ. Side population sorting separates subfractions of cycling and non-cycling intestinal stem cells. Stem cell research. 2014;12(2):364-75.
6. Buczacki SJ, Zecchini HI, Nicholson AM, Russell R, Vermeulen L, Kemp R, et al. Intestinal label-retaining cells are secretory precursors expressing Lgr5. Nature. 2013;495(7439):65-9.
7. Roth S, Franken P, Sacchetti A, Kremer A, Anderson K, Sansom O, et al. Paneth cells in intestinal homeostasis and tissue injury. PLoS One. 2012;7(6):e38965.
8. Sato T, van Es JH, Snippert HJ, Stange DE, Vries RG, van den Born M, et al. Paneth cells constitute the niche for Lgr5 stem cells in intestinal crypts. Nature. 2011;469(7330):415-8.
9. Hughes KR, Sablitzky F, Mahida YR. Expression profiling of Wnt family of genes in normal and inflammatory bowel disease primary human intestinal myofibroblasts and normal human colonic crypt epithelial cells. Inflamm Bowel Dis. 2011;17(1):213-20.
10. Kosinski C, Li VS, Chan AS, Zhang J, Ho C, Tsui WY, et al. Gene expression patterns of human colon tops and basal crypts and BMP antagonists as intestinal stem cell niche factors. Proc Natl Acad Sci U S A. 2007;104(39):15418-23.
11. Khor B, Gardet A, Xavier RJ. Genetics and pathogenesis of inflammatory bowel disease. Nature. 2011;474(7351):307-17.
12. Alkazmi LM, Dehlawi MS, Behnke JM. The mucosal cellular response to infection with Ancylostoma ceylanicum. Journal of helminthology. 2008;82(1):33-44.
13. Alkazmi LM, Behnke JM. The mucosal response of hamsters to a low-intensity superimposed secondary infection with the hookworm Ancylostoma ceylanicum. Journal of helminthology. 2011;85(1):56-65.
14. Patel N, Kreider T, Urban JF, Jr., Gause WC. Characterisation of effector mechanisms at the host:parasite interface during the immune response to tissue-dwelling intestinal nematode parasites. International journal for parasitology. 2009;39(1):13-21.
15. Ishikawa N, Wakelin D, Mahida YR. Role of T helper 2 cells in intestinal goblet cell hyperplasia in mice infected with Trichinella spiralis. Gastroenterology. 1997;113(2):542-9.
16. Kamal M, Wakelin D, Ouellette AJ, Smith A, Podolsky DK, Mahida YR. Mucosal T cells regulate Paneth and intermediate cell numbers in the small intestine of T. spiralis-infected mice. Clin Exp Immunol. 2001;126(1):117-25.
17. Walsh R, Seth R, Behnke J, Potten CS, Mahida YR. Epithelial stem cell-related alterations in Trichinella spiralis-infected small intestine. Cell Prolif. 2009;42(3):394-403.
18. Artis D, Grencis RK. The intestinal epithelium: sensors to effectors in nematode infection. Mucosal Immunol. 2008;1(4):252-64.
19. Dehlawi MS, Mahida YR, Hughes K, Wakelin D. Effects of Trichinella spiralis infection on intestinal pathology in mice lacking interleukin-4 (IL-4) or intestinal trefoil factor (ITF/TFF3). Parasitology international. 2006;55(3):207-11.
20. Foudi A, Hochedlinger K, Van Buren D, Schindler JW, Jaenisch R, Carey V, et al. Analysis of histone 2B-GFP retention reveals slowly cycling hematopoietic stem cells. Nat Biotechnol. 2009;27(1):84-90.
21. Beard C, Hochedlinger K, Plath K, Wutz A, Jaenisch R. Efficient method to generate single-copy transgenic mice by site-specific integration in embryonic stem cells. Genesis (New York, NY : 2000). 2006;44(1):23-8.
22. Wakelin D, Lloyd M. Immunity to primary and challenge infections of Trichinella spiralis in mice: a re-examination of conventional parameters. Parasitology. 1976;72(2):173-82.
23. Ishikawa N, Goyal PK, Mahida YR, Li KF, Wakelin D. Early cytokine responses during intestinal parasitic infections. Immunology. 1998;93(2):257-63.
24. Hughes KR, Mahida YR. Determination of Histone 2B-Green Fluorescent Protein (GFP) Retention in Intestinal Stem Cells. Methods in molecular biology (Clifton, NJ). 2018;1686:79-89.

25. Potten CS, O'Shea JA, Farrell CL, Rex K, Booth C. The effects of repeated doses of keratinocyte growth factor on cell proliferation in the cellular hierarchy of the crypts of the murine small intestine. Cell Growth Differ. 2001;12(5):265-75.
26. Bromley M, Rew D, Becciolini A, Balzi M, Chadwick C, Hewitt D, et al. A comparison of proliferation markers (BrdUrd, Ki-67, PCNA) determined at each cell position in the crypts of normal human colonic mucosa. Eur J Histochem. 1996;40(2):89-100.
27. Potten CS, Owen G, Roberts SA. The temporal and spatial changes in cell proliferation within the irradiated crypts of the murine small intestine. Int J Radiat Biol. 1990;57(1):185-99.
28. Gandara RM, Mahida YR, Potten CS. Regional differences in stem and transit cell proliferation and apoptosis in the terminal ileum and colon of mice after 12 Gy. International journal of radiation oncology, biology, physics. 2012;82(3):e521-8.
29. Montgomery RK, Carlone DL, Richmond CA, Farilla L, Kranendonk ME, Henderson DE, et al. Mouse telomerase reverse transcriptase (mTert) expression marks slowly cycling intestinal stem cells. Proc Natl Acad Sci U S A. 2011;108(1):179-84.
30. Elphick DA, Mahida YR. Paneth cells: their role in innate immunity and inflammatory disease. Gut. 2005;54(12):1802-9.
31. Howitt MR, Lavoie S, Michaud M, Blum AM, Tran SV, Weinstock JV, et al. Tuft cells, taste-chemosensory cells, orchestrate parasite type 2 immunity in the gut. Science. 2016;351(6279):1329-33.
32. Gerbe F, Sidot E, Smyth DJ, Ohmoto M, Matsumoto I, Dardalhon V, et al. Intestinal epithelial tuft cells initiate type 2 mucosal immunity to helminth parasites. Nature. 2016;529(7585):226-30.
33. Yan KS, Chia LA, Li X, Ootani A, Su J, Lee JY, et al. The intestinal stem cell markers Bmi1 and Lgr5 identify two functionally distinct populations. Proc Natl Acad Sci U S A. 2012;109(2):466-71.
34. Martinez Rodriguez NR, Eloi MD, Huynh A, Dominguez T, Lam AH, Carcamo-Molina D, et al. Expansion of Paneth cell population in response to enteric Salmonella enterica serovar Typhimurium infection. Infect Immun. 2012;80(1):266-75.
35. Cliffe LJ, Humphreys NE, Lane TE, Potten CS, Booth C, Grencis RK. Accelerated intestinal epithelial cell turnover: a new mechanism of parasite expulsion. Science. 2005;308(5727):1463-5.

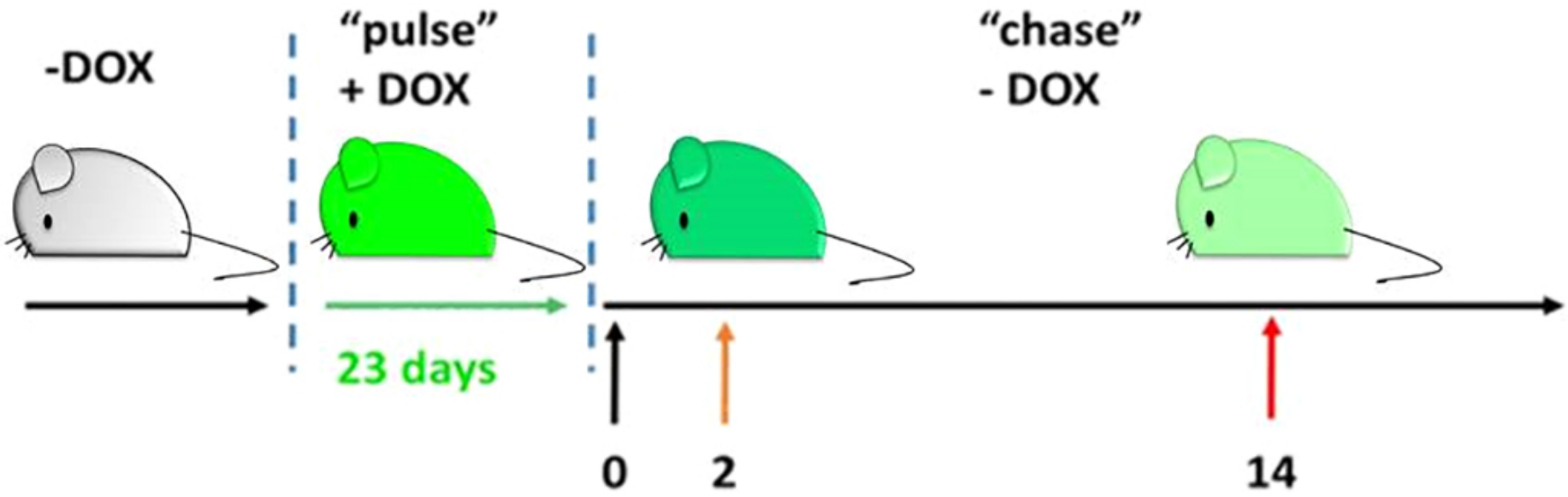

Figure 1

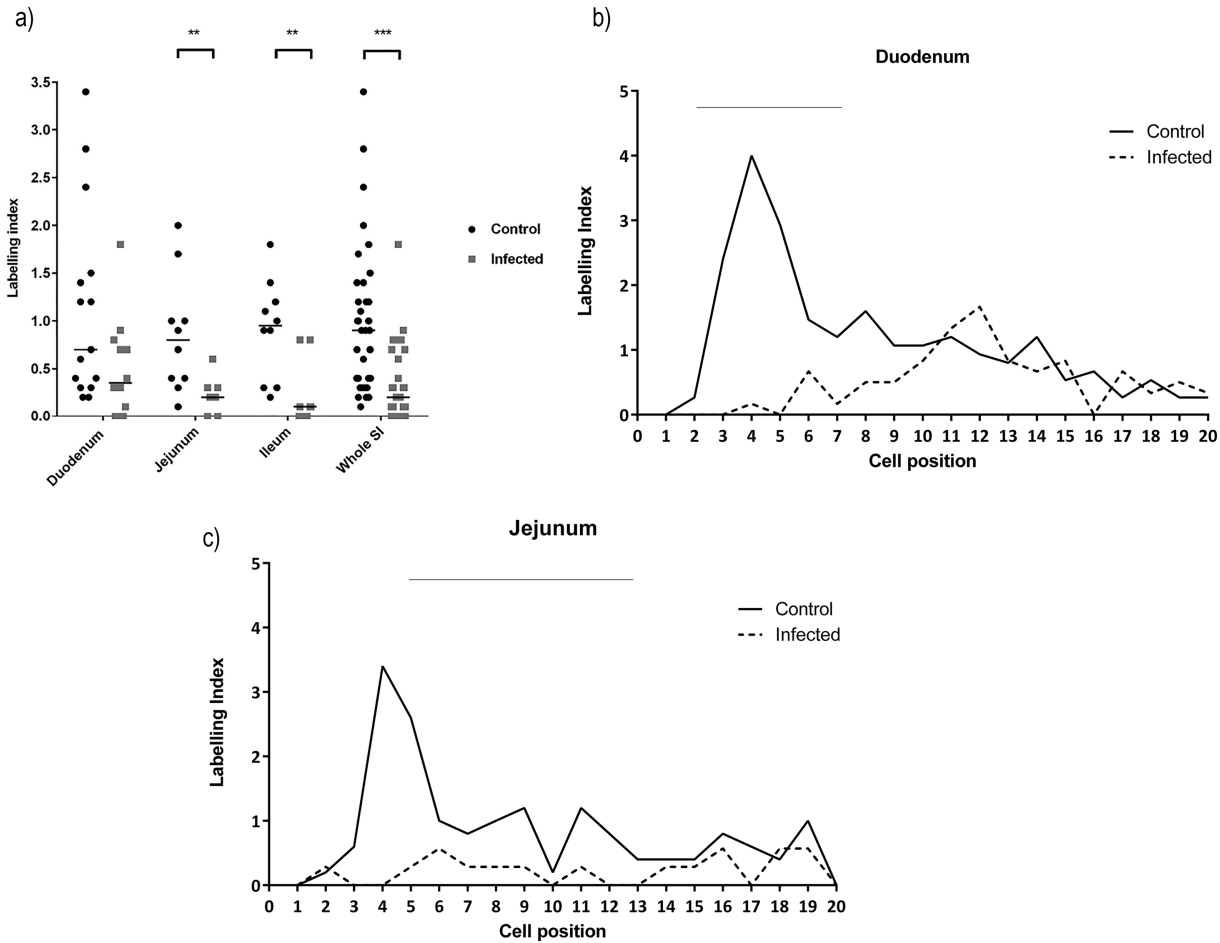
a)
**
**
***
Labelling index
3.5
3.0
2.5
2.0
1.5
1.0
0.5
0.0
Duodenum
Jejunum
Ileum
Whole SI
Control
Infected
b)
Duodenum
Labelling Index
Cell position
Control
Infected
c)
Jejunum
Labelling Index
Cell position
Control
Infected

Figure 2A

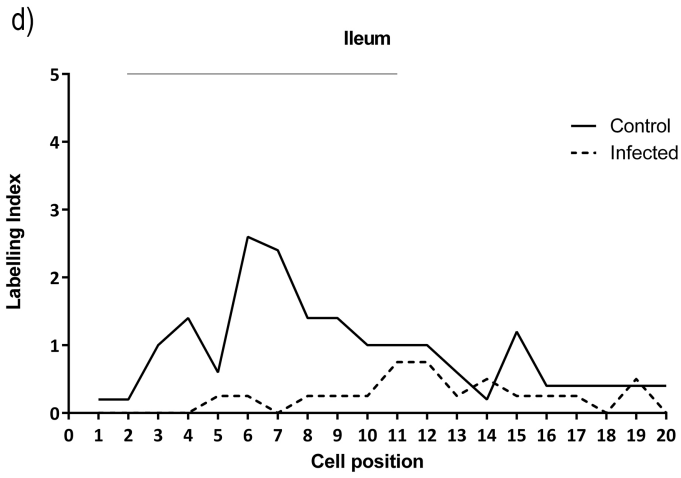
d)
Ileum
Labelling Index
Cell position
Control
Infected
0
1
2
3
4
5
0 1 2 3 4 5 6 7 8 9 10 11 12 13 14 15 16 17 18 19 20

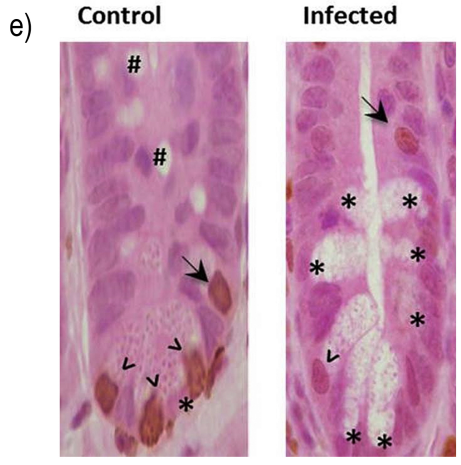
e)
Control
Infected

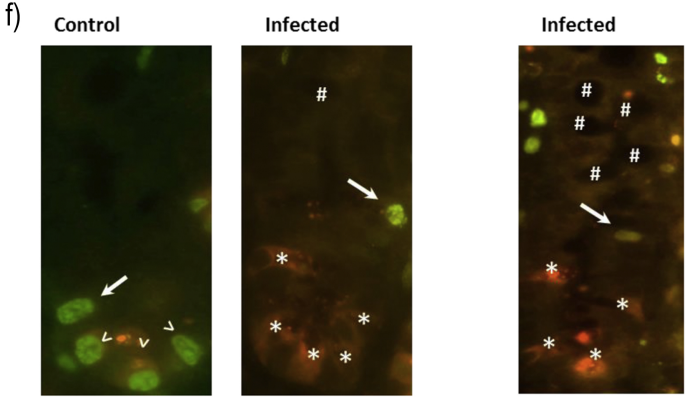
f)
Control
Infected
Infected

Figure 2B

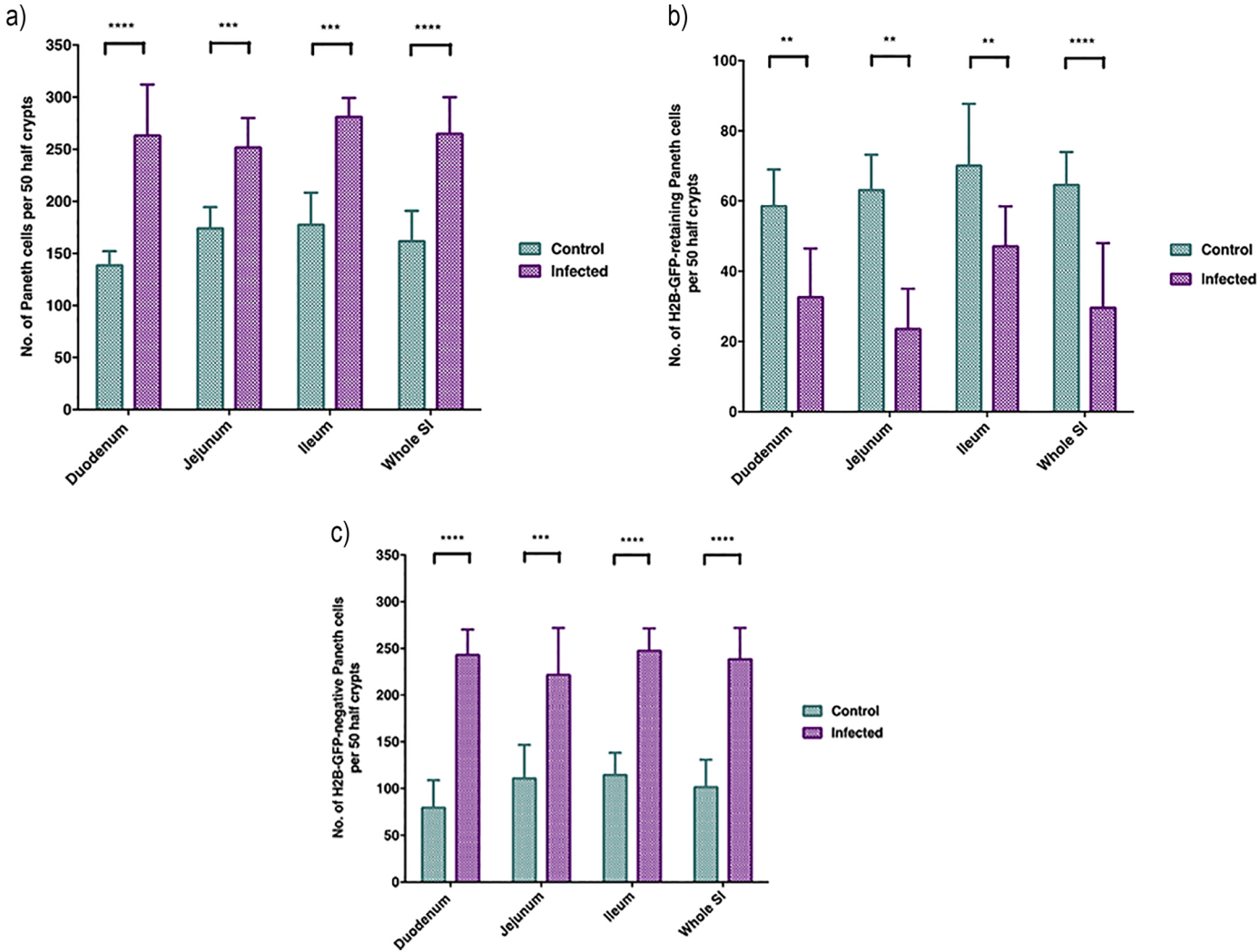
a)
No. of Paneth cells per 50 half crypts
350
300
250
200
150
100
50
0
****
***
***
****
Duodenum
Jejunum
Ileum
Whole SI
Control
Infected
b)
No. of H2B-GFP-retaining Paneth cells per 50 half crypts
100
80
60
40
20
0
**
**
**
****
Duodenum
Jejunum
Ileum
Whole SI
Control
Infected
c)
No. of H2B-GFP-negative Paneth cells per 50 half crypts
350
300
250
200
150
100
50
0
****
***
****
****
Duodenum
Jejunum
Ileum
Whole SI
Control
Infected

Figure 3

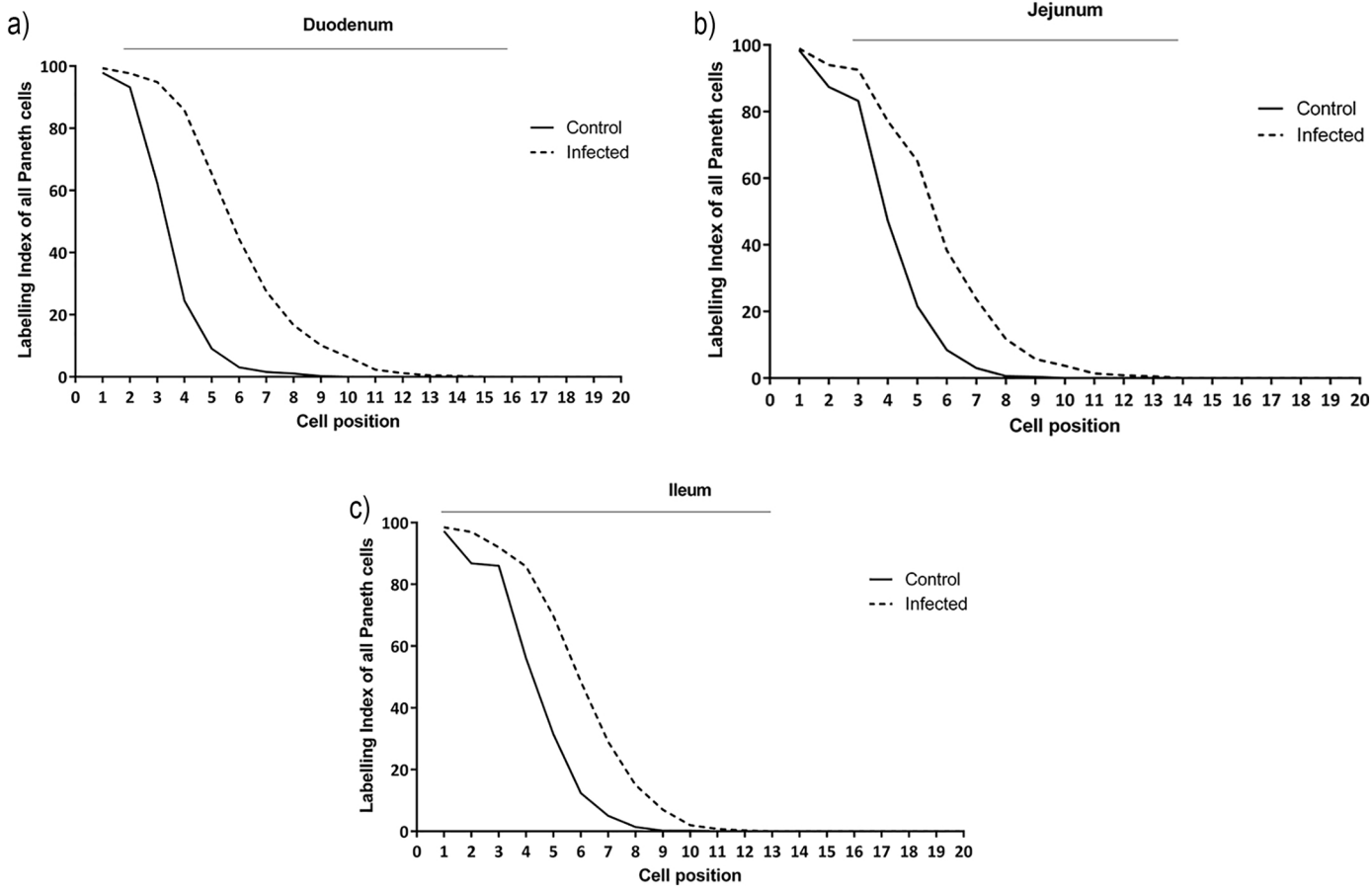
a)
Duodenum
Labelling Index of all Paneth cells
Cell position
Control
Infected
b)
Jejunum
Labelling Index of all Paneth cells
Cell position
Control
Infected
c)
Ileum
Labelling Index of all Paneth cells
Cell position
Control
Infected

Figure 4

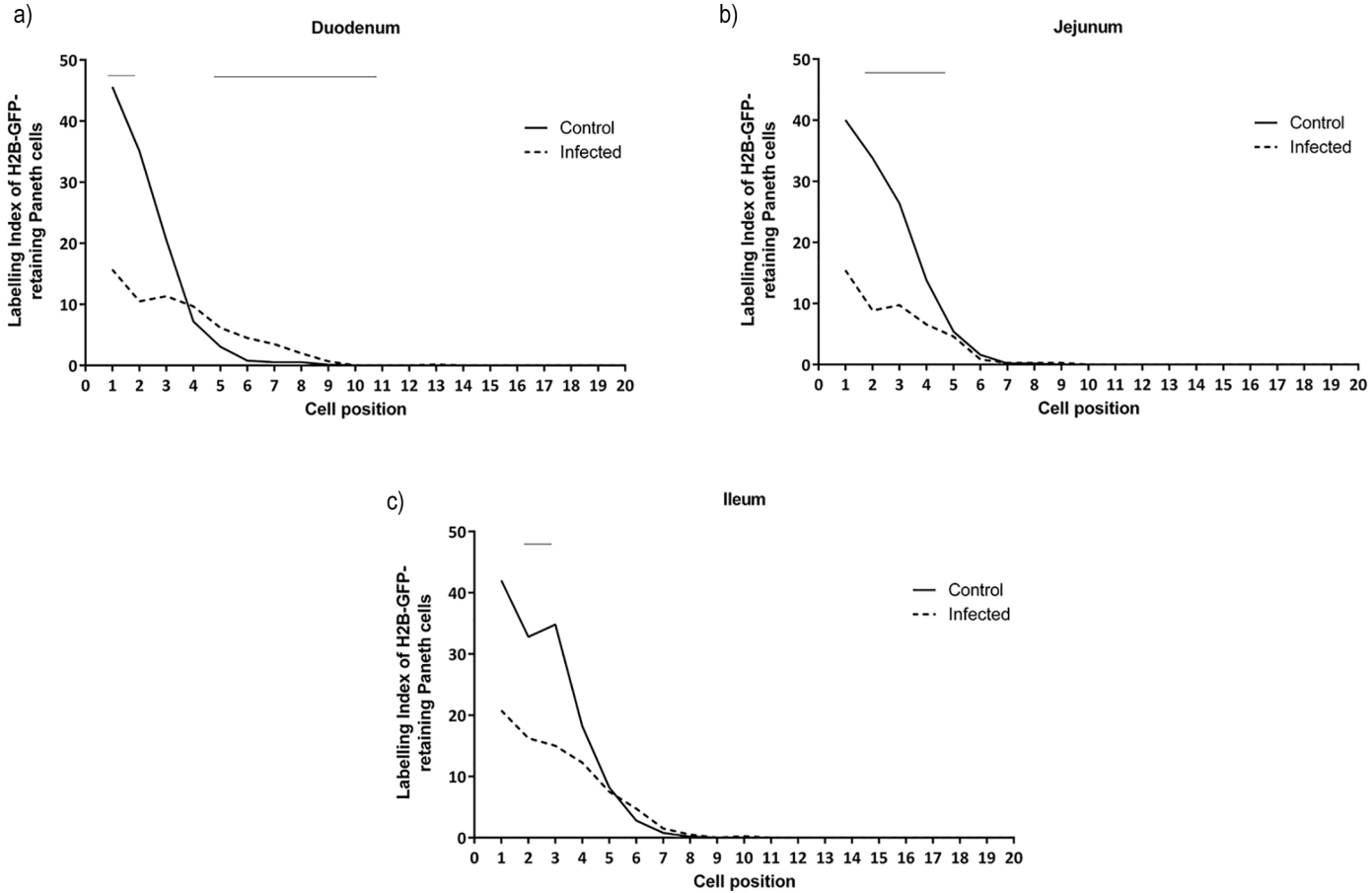
a)
Duodenum
Labelling Index of H2B-GFP-retaining Paneth cells
Control
Infected
Cell position
b)
Jejunum
Labelling Index of H2B-GFP-retaining Paneth cells
Control
Infected
Cell position
c)
Ileum
Labelling Index of H2B-GFP-retaining Paneth cells
Control
Infected
Cell position

Figure 5

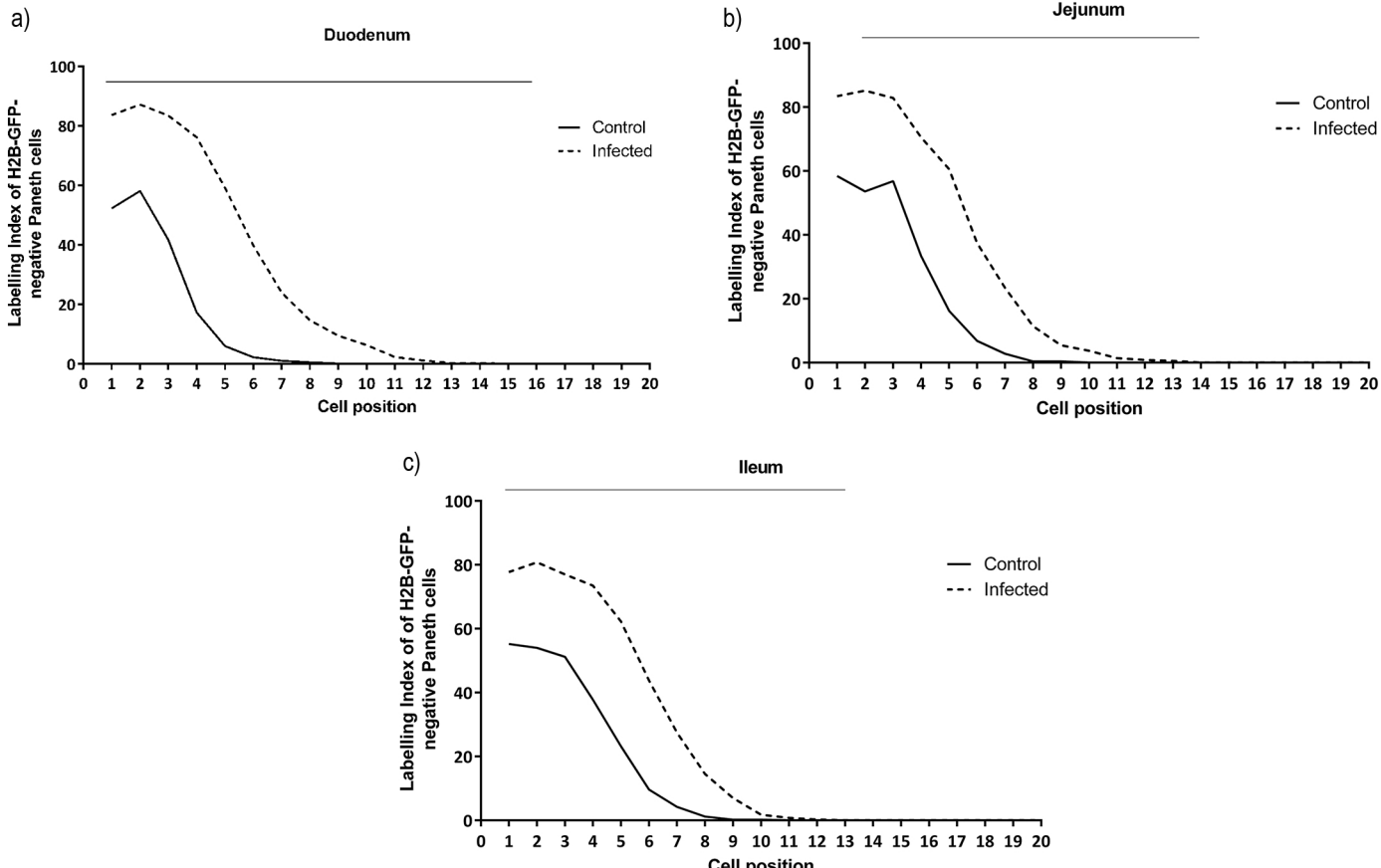
a)
Duodenum
Labelling Index of H2B-GFP-negative Paneth cells
Cell position
Control
Infected
b)
Jejunum
Labelling Index of H2B-GFP-negative Paneth cells
Cell position
Control
Infected
c)
Ileum
Labelling Index of of H2B-GFP-negative Paneth cells
Cell position
Control
Infected

Figure 6

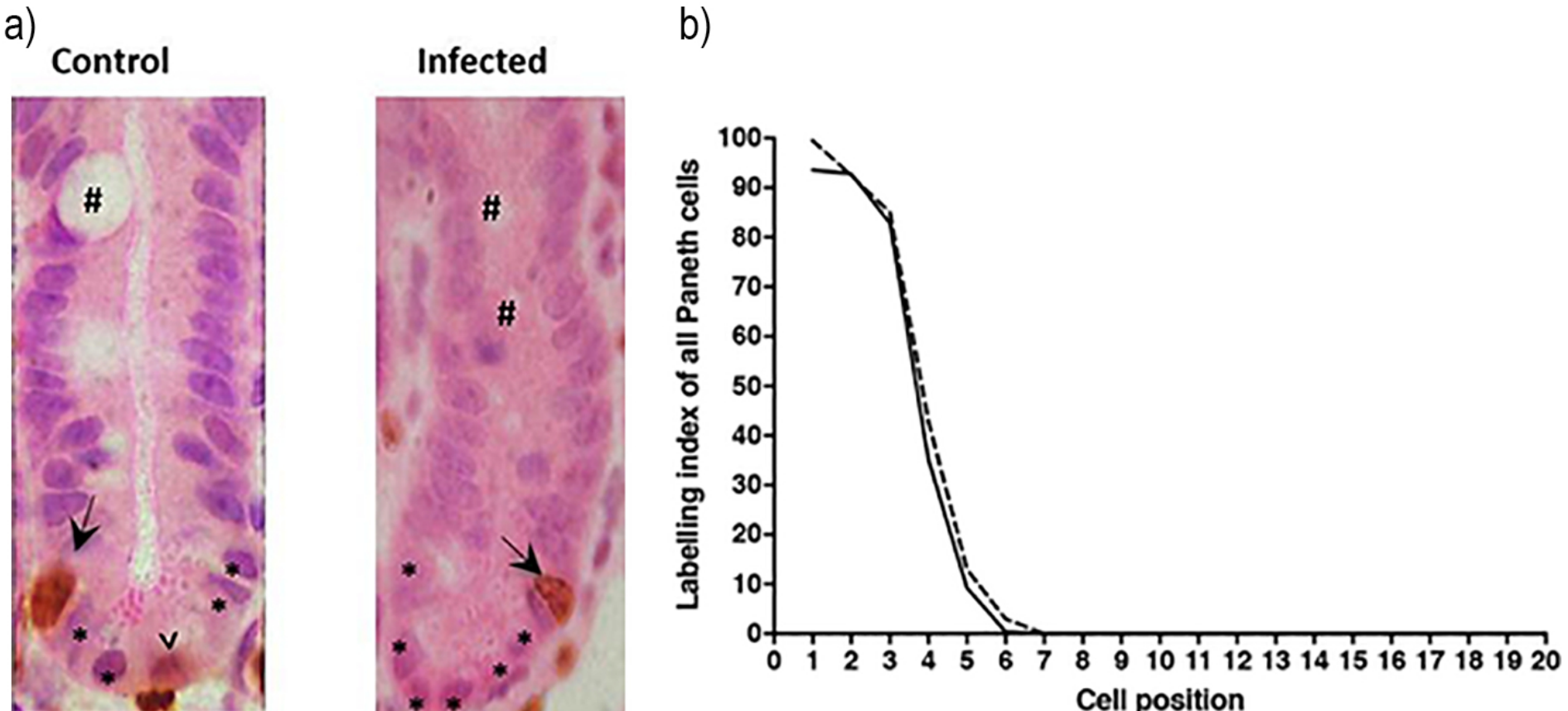
a)
Control
Infected
#
#
#
b)
Labelling index of all Paneth cells
100
90
80
70
60
50
40
30
20
10
0
0 1 2 3 4 5 6 7 8 9 10 11 12 13 14 15 16 17 18 19 20
Cell position

Figure 7